الجمـــهوريـــة الجـــزائريـــة الديـمقـراطيـــــــة الشـعبيـــــة
PEOPLE'S DEMOCRATIC REPUBLIC OF ALGERIA
وزارة التعـلـيـم الـعـالـــي والـبـحـث الـعـلـمي
MINISTRY OF HIGHER EDUCATION AND SCIENTIFIC RESEARCH
جـامـعـة عمّـــار ثـلـيـــجـــي بالأغـــواط
UNIVERSITY AMAR TELIDJI LAGHOUAT
كـلـيـــــة الـعـلـــــوم
FACULTY OF SCIENCES
قسم عـلـــــوم المادة
Department OF Material Sciences

Field : Physics

Option : Applied Physics

Master thesis presented

by:

BAGUA ELHAOUAS

THEME

Theoretical study on the CaH_6system

Sustained before a jury composed of:

Mr. HALIT Mohamed	*M.C.A*	*President*
Mr. KHENCHOUL Salah	*M.C.B*	*Supervisor*
Mr. BENGHIA Ali	*PhD stud*	*co-supervisor*
Mr. ARAR Rabie	*M.A.A*	*Examiner*
Mrs. HAMDI Roukia	*M.A.A*	*Examiner*

University year 2017-2018

Dedication

Dedicate this work to my precious parents, and my family

Dedicate to all my wonderful teachers and professors

Dedicate to all my friends

Dedicate To all who have sacrificed their time for science.

And to all who have used science for good.

And the prosperity of humanity.

ELHAOUAS

ACKNOWLEDGEMENTS

First thanks are to Allah, we praise him and to inspire the patients in this research.

First, I would like to express my deepest thanks to my supervisor ***Mr. Khenchoul Salah*** *who did me the honor to carry out this work under his direction, for his great patience, his availability and his judicious advice and co-supervisor*

Mr. BENGHIA Ali. *And I would like to thank in particular*

Mr. LAGOUN Brahim *for his constant support and advices, which I benefited from.*

I thank jury president ***Mr. HALIT Mohamed*** *and jury Members* ***Mrs. HAMDI Roukia*** *and* ***Mr. ARAR rabie*** *For kindly accepting to be part of the jury and consider my work.*

This work was done at the Research Laboratory of the University of Laghouat. To this end, I would like to express my sincere gratitude and my thanks to the Director of the laboratory ***Mr. LEFKAIR Ibn khaldoun.***

And with gratitude to the University Administration AMAR TELIDJI LAGHOUAT to provide research resources.

Thanks to M.FADLA, Z.ABI ISMAIL, S.SARHANI, M.HIDBI,

And thank all those who helped me in my research this and forgot to mention his name, even by small advice.

Table of Contents

Chapter I: superconducting materials

Chapter II: Ab-initio methods

Chapter III. Results and Discussions

TABLES OF FIGURES

LIST OF TABLES

Introduction

General Introduction

Superconductivity is a spectacular phenomena that always fascinates scientific community. A century after its discovery in 1911 by Kammerlingh Onnes in mercury [1], the material immersed in the superconducting state below its superconducting phase transition temperature, or critical temperature, has two remarkable properties: it leads the electric current without any resistance, that is to say without dissipation, and it expels completely the magnetic flux, phenomenon called Meissner effect [2]. It 1957 Bardeen, Cooper and Schrieffer have proposed the BCS theory [3] to explain the microscopic characteristics of this new state of matter. However, this theory predicted a theoretical maximum to T_c of around 30-40 K, as above this, thermal energy would cause electron-phonon interactions of an energy too high to allow formation of or sustain Cooper pairs. The discovery of high temperature superconductors in 1986 [4] which broke this limit and put it down debate as to what mechanism prevails at higher temperatures, as BCS cannot account for this, as for the cuprates and in the recently discovered iron-based superconductor family.

The discovery of new families of the hydrogen-rich superconductors [4] which stabilized at high-pressure conditions have been the subject of topic interests. There is an essential hope that hydrogen-rich superconductors are promising candidates of room-temperature superconductors. A lot of theoretical simulations yielding very high superconducting temperatures were made after that predictions (see recent references [6,7]).

Recent advances in first-principles crystal structure prediction techniques have opened up the possibility of reliable prediction of superconductive structures, and subsequent superconductivity calculations based on phonon-mediated superconducting mechanism revealed a general appearance of high temperature superconductivity in pressurized hydrides. Theory-orientated experiments at high pressure discovered a number of hydrogen-rich superconductors, among which clathrate calcium hydride at high pressures; exhibit a remarkably high superconducting critical temperature reaching 220–235 K at 150 GPa. In this manuscript, we discuss the emerging research activities towards hydrogen-rich superconductors at high pressures and outlook the future direction in the field

The aim of this thesis is to achieve a better understanding of the structural, electronic, and vibrational properties under pressure of cI14- CaH_6 phases by using the ab initio calculations in the framework of density functional theory (DFT) employing ABINIT software [8].

The manuscript is organized in three chapters. In the first chapter, the notion of superconductivity is introduced in a general way. Superconductors based on calcium hydride clathrate at high pressures. The second chapter contains the theoretical foundations of density functional theory (DFT), which is one of the ab-initio methods for predicting the properties of materials. The third chapter presents the results of our calculations with a parallel discussion and a comparison of these with the results of other and theoretical works.

References

[1] H. Kamerlingh Onnes. Commun. Phys. Lab. Univ. Leiden. Suppl., 1911.

[2] W. Meissner and R. Ochsenfeld. Naturwiss, 21 : 787–788, 1933.

[3] J. J. Bardeen, L. N. Cooper, and J. R. Schrieffer. Phys. Rev. 108 : 1175, 1957.

[4] M. K. Wu, J. R. Ashburn, C. J. Torng, P. H. Hor, R. L. Meng, L. Gao, Z. J. Huang, Y. Q. Wang, et C. W. Chu. Physical Review Letters 58(9), 908–910. 1987

[5] H. Wang, J. S. Tse, K. Tanaka, and Y. Ma, *Proc. Natl. Acad. Sci.*, vol. 109, 17, 2012.

[6] D.Duan, et al, Sci. Reports 4, 6968, 2014.

[7] Y.Li, J. Hao, & Ma, Y, J. Chem. Phys. 140, 174712, 2014.

[8] X. Gonze, et al, *Z. Kristallogr*. **220**, 558, 2005.

Chapter I:

Superconducting materials

Chapter I: Superconducting materials

I.1 Introduction:

The outline of this chapter introduce the fundamental properties of superconductors and some basic theories including different aspects of physics in this kind of materials. The last part deal mainly with compound CaH6.

I.2 Brief history:

Ever since the discovery of superconductivity in 1911 [1], it has been one of the most intriguing puzzles in the field of condensed matter physics. He observed that the electrical resistance of mercury vanishes at around 4.2 K. The best-known features of the superconducting materials are zero electrical resistance and complete expulsion of the magnetic field inside the material (both taking place at finite temperature)[2]. The phenomena of perfect conductivity below a critical temperature T_c which is known as the superconducting transition temperature is a characteristic feature for all superconductors. In addition, the conventional superconductors also exhibit perfect diamagnetism below this temperature T_c. This phenomenon, known as Meissner effect, was discovered by Meissner and Ochsenfeld in 1933 [3]. They discovered that, not only is. the magnetic field excluded from the superconductor, it is expelled out when it is cooled below T_c. In a magnetic field, screening currents are generated that flow through the surface of the superconductor and cancels the flux density within it. There is also a critical field, H_c, beyond which flux can enter into the superconductor. H_c is related thermodynamically to the difference in free energy of the normal and superconducting states in zero field.

Almost ten years later in 1957 year Bardeen, Cooper and Schrieffer published a microscopic theory of superconductivity (BCS theory) [4]. The key idea was a pairing of electrons. BCS theory states that below critical temperature it's energetically more preferable that two electrons with opposite spin and momenta will form a pair. Such pair of electrons can be considered as a new particle, and it's called Cooper pair. Cooper pair has a zero spin and appears to be a boson. The understanding of the phenomenon of superconductivity did not lead to a quick progress in finding of materials with higher *Tc*. The BCS theory does not have a real predicted power.

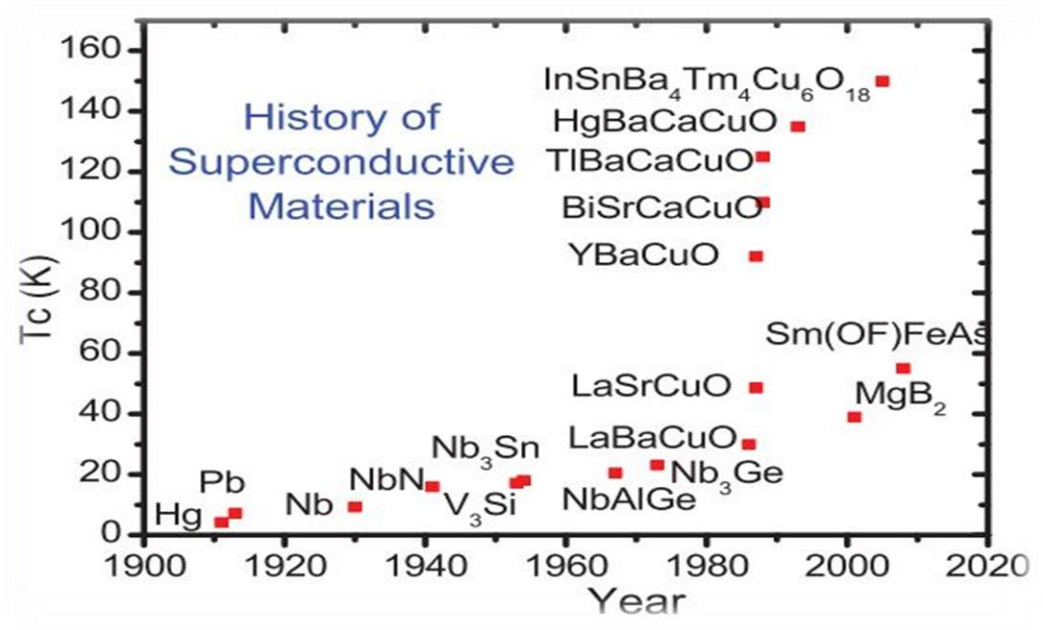

Figure I.1 Survey diagram for superconductive materials[5].

I.3 Basic notions of superconductivity:

I .3.1 Zero resistivity:

The most renowned property of superconductors is the absence of electrical resistance below the critical temperature T_c, (see Fig. **I.1**). Zero resistance implies that a small current sent through the material will not be affected by any power losses at all. This phenomenona cannot be described by the ordinary Maxwell's equations for electromagnetism, they must instead be modified to include superconductivity[6].

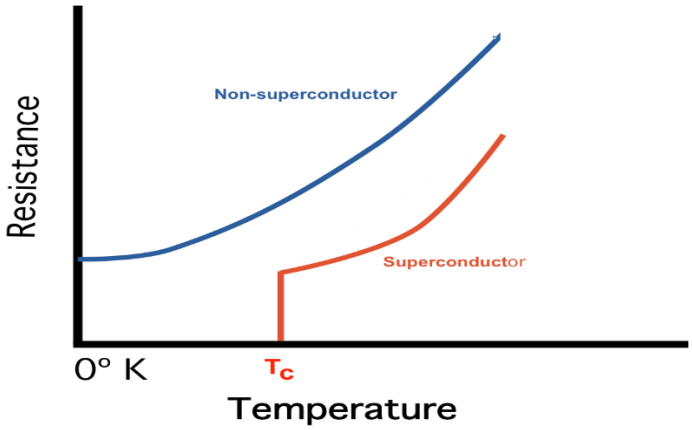

Figure I.2. The phase transition between the superconductor phase and the normal conductor phase.

I .3.2 The Meissner effect:

The Meissner effect was discovered by Meissner and Ochsenfeld [7] , 22 years after the discovery of superconductivity by Onnes. Thereafter, the state of superconductivity is considered to be a thermodynamic phenomenona, since its state is defined by thermodynamic variables such as temperature *T* and applied magnetic field *H*. In general, type-I superconducting materials possess the following two properties:

• Property of perfect conductor ρ=0.

• Property of perfect diamagnetism $\chi = \frac{dM}{dH} = -1$ (I.1)

The perfect diamagnetism or Meissner effect is due to a shielding current which develops on the surface of the superconductor when in the presence of an applied magnetic field *H* [8].

The property of expulsion of the magnetic flux in a superconductor is known as the *Meissner effect*. (See Fig. I.2).

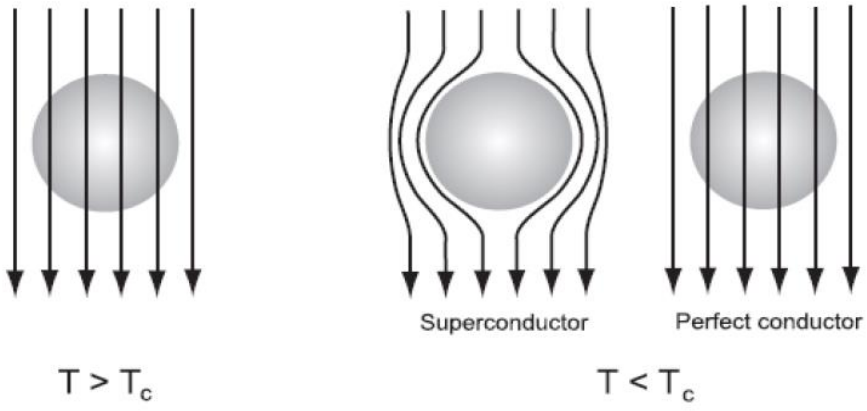

Figure I.3. In the presence of an external field H < H_c, a superconductor expels the magnetic flux when cooled below T_c, while in a perfect conductor the flux would remain the same.

Figure from Espinosa-Arronte [9].

A popular experiment showing the Meissner effect is to put an ordinary magnet on a superconductor at room temperature and then cool it below the critical temperature. Above T_c the magnetic flux from the magnet penetrates the superconductor but when T_c is reached all the magnetic flux is forced out of the superconductor, which then lifts the magnet from the superconductor, making it float above it.

I .3.3 The different types of superconductors:

Very early on, magnetization measurements showed that the superconducting phase existed in a limited range, not only of temperature but also of magnetic field. After much confusion and convicting experimental results, it was finally the theoretical analysis of A. Abrikosovin 1957 that showed that superconductivity could disappear via two distinct scenarios, thus leading to the classification of superconducting materials into those of type I and of type II. In a superconductor of type I, the superconductivity vanishes abruptly at a critical value H_c of the field. H_c is always small, with $\mu_0 H_c$ no more than 0.1 tesla. Only pure elemental superconductors (with a few exceptions, such as Niobium), are of type I. In a type II superconductor, there is no discontinuity to be seen, but rather a gradual weakening of the magnetic response starting from a lower critical magnetic field H_{c1} [10].

Complete suppression of superconductivity occurs only when the field reaches an upper critical value H_{c2} which can be very high ($\mu_0 H_{c2}$ may be several tens of, or even a hundred, teslas). Superconducting compounds and alloys are all of type II.

I .3.4.1 Superconductors of type I:

The magnetic field, which destroys the superconductivity of the type-I material is referred to as "thermodynamic critical field B_C". Its variation as a function of temperature for several materials is nearly parabolic (see Fig. 1.3):

$$B_C = B_0 \left[1 - \left(\frac{T}{T_C}\right)^2\right] \qquad \text{(I.2)}$$

Where B_0 represents the extrapolated value of BC at T = 0K. In the international system, the magnetic field B (in teslas) which prevails in the material is given by the following relation:

$$B = \mu_0 (H + M) \qquad \text{(I.3)}$$

Where **M** is the magnetization of the sample in A/m, **H** the field of excitation in A/m and m0 the magnetic permeability of the vacuum. The Meissner state corresponds in the case where **B** = **0** leading to **M** = – **H**: the diamagnetism is therefore perfect until the critical field B_C above which the material becomes normal, so **M** = **0** (see Fig. 1.4) [11].

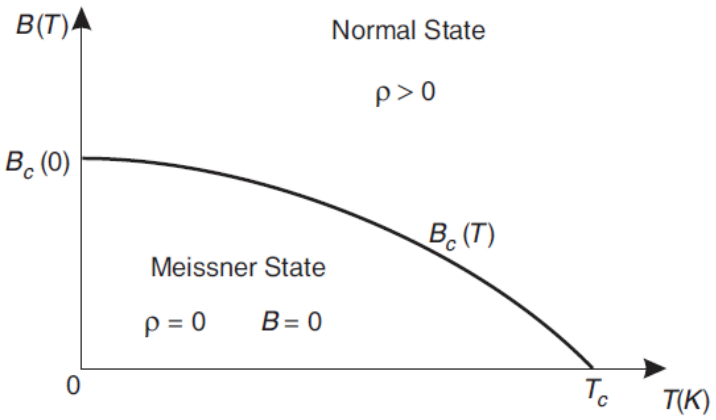

Figure I.4. Phases diagram of a type-I superconductor.

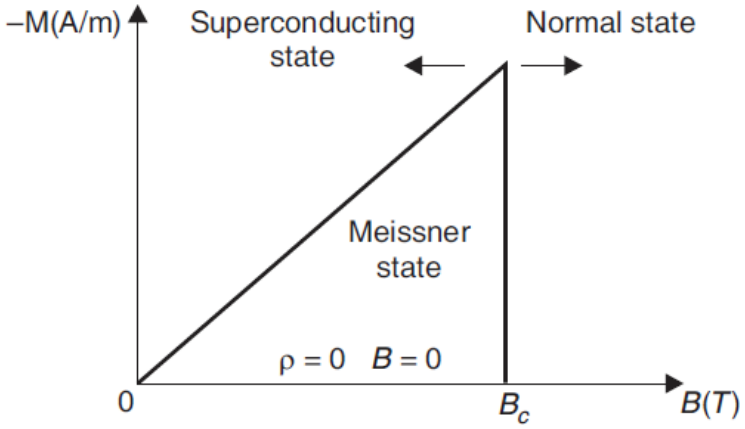

Figure I.5. Magnetization as a function of the magnetic field of a type-I superconductor. The Meissner state is characterized by a perfect diamagnetism.

I .3.4.2 Superconductors of type II:

A type-II superconductor has two critical fields, the lower critical field $B_{C1}$and the upper critical field B_{C2}. For magnetic fields lower than B_{C1}, the type- II superconductor behaves like a type-I superconductor below B_C: it totally expels the magnetic flux (see Fig. 1.**6**) [11].

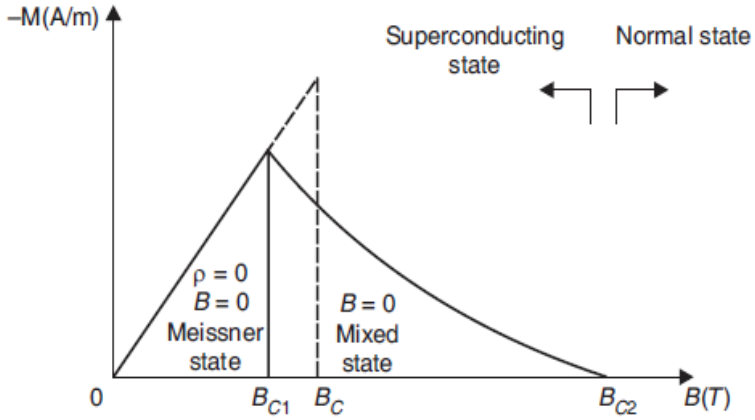

Figure I.6. Magnetization as a function of the magnetic field of a type-II superconductor. In the mixed state, the Meissner effect is partial.

Type II superconductors are the most technologically useful because the second critical field can be quite high, enabling high field electromagnets to be made out of superconducting wire.

Wires made from say niobium-tin (Nb3Sn) have a B_{c2} as high as 24.5 Tesla – in practice it is lower. This makes them useful for applications requiring high magnetic fields, such as Magnetic Resonance Imaging (MRI) machines. The advantage of using superconducting electromagnets is that the current only has to be applied once to the wires, which are then formed into a closed loop and allow the current (and field) to persist indefinitely – as long as the superconductor stays below the critical temperature. That is, the external power supply can be switched off . As a comparison, the strongest permanent magnets today may be able to produce a field close to 1Tesla. However, it is possible to obtain up to 24.5 Tesla from a Niobium–Tin superconductor[12].

I.4 High temperature superconductors:

The key question about high-critical temperature superconductivity is the variation of the critical temperature T_C with the material characteristics. In the recent years, several models have been proposed in order to explain the high value of T_C. Even though these models are not unanimously agreed upon within the scientific community, it is not less true that they partly predict the variations of certain parameters. The most realistic theories seem to be those, which refine or modify the already existing classical theories (London model, Ginzburg-Landau theory, BCS theory). Of the many surprising facts which have appeared with these new materials , an unusual irreversibility line in the H-T plane with a possible fusion of the vortices lattice above this line, an enormous non exponential relaxation time of the magnetic properties and its ageing effects, a

disagreement in the estimation of the critical current densities, an almost exponential decrease of the critical current density as a function of the temperature and the field, an anomaly in the profile of the variation of the susceptibility as a function of the field, an unforeseen widening of the resistive transition under field and many others [11].

I.5 Equations for calculating T_C:

At the first stage of self-consistent procedure of the numerical solution of the Eliashberg equation [13] we calculated Fredholm kernels of electron-phonon interaction $I_1(\omega,\omega')$, $I_1(\omega,\omega')$, $I_2(\omega,\omega')$. Integration was divided into intervals using the following symmetry properties

$\Delta(-\omega) = \Delta^*(\omega)$, $Z(-\omega) = Z^*(\omega)$, $\alpha 2(-\omega)F(-\omega) = \alpha 2(\omega)F(\omega)$ [14], but avoiding points T = 0 K,

ω =0 Ry due to possible divergences of 1/T, 1/ω, ω/T during numerical integration :

$$I_1(\omega,\omega') = \int_0^\infty a^2(\Omega)F(\Omega).\left\{\frac{\left(\exp\left(-\frac{\hbar\omega'}{KT}\right)+1\right)^{-1}+\left(\exp\left(\frac{\hbar\Omega}{KT}\right)-1\right)^{-1}}{\hbar\omega'+\hbar\Omega-\hbar\omega}+\frac{\left(\exp\left(\frac{\hbar\omega'}{KT}\right)+1\right)^{-1}+\left(\exp\left(\frac{\hbar\Omega}{KT}\right)-1\right)^{-1}}{\hbar\omega'-\hbar\Omega-\hbar\omega}\right\}.\hbar d\Omega \qquad \text{(I.4)}$$

$$I_{-1}(\omega,\omega') = \int_0^\infty a^2(\Omega)F(\Omega).\left\{\frac{\left(\exp\left(\frac{\hbar\omega'}{KT}\right)+1\right)^{-1}+\left(\exp\left(\frac{\hbar\Omega}{KT}\right)-1\right)^{-1}}{-\hbar\omega'+\hbar\Omega-\hbar\omega}-\frac{\left(\exp\left(-\frac{\hbar\omega'}{KT}\right)+1\right)^{-1}+\left(\exp\left(\frac{\hbar\Omega}{KT}\right)-1\right)^{-1}}{\hbar\omega'+\hbar\Omega+\hbar\omega}\right\}.\hbar d\Omega \qquad \text{(I.5)}$$

$$\frac{I_2(\omega,\omega')}{\hbar\omega} = \int_0^\infty 2a^2(\Omega)F(\Omega).\left\{\frac{\left(\exp\left(\frac{\hbar\omega'}{KT}\right)+1\right)^{-1}+\left(\exp\left(\frac{\hbar\Omega}{KT}\right)-1\right)^{-1}}{(\hbar\omega)^2-(\hbar\Omega-\hbar\omega')^2}-\frac{\left(\exp\left(-\frac{\hbar\omega'}{KT}\right)+1\right)^{-1}+\left(\exp\left(\frac{\hbar\Omega}{KT}\right)-1\right)^{-1}}{(\hbar\Omega-\hbar\omega')^2-(\hbar\omega)^2}\right\}.\hbar d\Omega \qquad \text{(I.6)}$$

Where μ^* is the pseudopotential of Coulomb and ω is a Cutoff frequency

Then, we calculated the Coulomb contribution to the order parameter using common expression for electronic density of states in BCS theory [13]:

$$I_3 = -\mu.\int_0^\infty \mathrm{Re}\left(\frac{\Delta(\omega')}{\sqrt{\hbar^2\omega'^2-\Delta^2(\omega')}}\right).\frac{\exp\left(\frac{\hbar\omega'}{KT}\right)-1}{\exp\left(\frac{\hbar\omega'}{KT}\right)+1}.\hbar d\omega' \qquad \text{(I.7)}$$

Calculation of average Coulomb electron-electron repulsion was performed using the upper bound of empirical value μ* = 0.1 (0.15) with ωc = 75 THz = 0.31 eV (upper bound of phonon spectrum) and *Ee* = 85 eV [15].

$$\mu = \frac{\mu^*}{1 - \mu^* \ln \frac{E_e}{\hbar \omega_C}} \tag{I.8}$$

Where E is the characteristic electron energy.

Then, a function of electron mass renormalization Z (ω) was calculated as

$$Z(\omega) = 1 - \int_0^\infty \mathrm{Re}\left(\frac{\hbar\omega'}{\sqrt{\hbar^2\omega'^2 - \Delta^2(\omega')}} \right) . \frac{I_2(\omega,\omega')}{\hbar\omega} . \hbar d\omega' \tag{I.9}$$

After that the next approximation for the order parameter (or the value of superconducting gap, Δ(ω))

$$\Delta(\omega) = \frac{I_3 + \int_0^\infty \mathrm{Re}\left(\frac{\Delta(\omega')}{\sqrt{\hbar^2\omega'^2 - \Delta^2(\omega')}} \right) \cdot I_1(\omega,\omega') . \hbar d\omega' + \int_0^\infty \mathrm{Re}\left(\frac{\Delta(\omega')}{\sqrt{\hbar^2\omega'^2 - \Delta^2(\omega')}} \right) \cdot I_{-1}(\omega,\omega') . \hbar d\omega'}{Z(\omega)} \tag{I.10}$$

And the new $I_1(\omega,\omega')$, $I_1(\omega,\omega')$, $I2(\omega,\omega')$ integrals are calculated. Then, the next iteration for Δ(ω) is calculated and the new cycle starts again. Value of Δ(ω) obtained after 10-20 iterations was used for construction of $\Delta(T, \omega)|\omega \to 0 = \Delta(T)$ function and search for Tc ($\Delta(Tc) \to 0$) as well as characteristic ratio 2Δ(0)/Tc and its deviation from weak coupling limit (3.52).

The superconducting transition temperature T_C was estimated by using two equations: "full" – Allen-Dynes and "short" – modified McMillan equation. The “full” Allen-Dynes equation for calculating T_C has the following form [15]:

$$T_C = \omega_{\log} \frac{f_1 f_2}{1.2} \exp\left(\frac{-1.04(1+\lambda)}{\lambda - \mu^* - 0.62\lambda\mu^*} \right) \quad \text{(I.11)}$$

While the modified McMillan equation has the form as:

$$T_C = \frac{\omega_{\log}}{1.2} \exp\left(\frac{-1.04(1+\lambda)}{\lambda - \mu^* - 0.62\lambda\mu^*} \right) \quad \text{(I.12)}$$

The EPC constant λ and logarithmic average frequency ω_{log} were calculated as:

$$\lambda = \int_{\omega_{\min}}^{\omega_{\max}} \frac{2\alpha^2 F(\omega)}{\omega} d\omega \quad \text{(I.13)}$$

and

$$\omega_{\log} = \exp\left(\frac{2}{\lambda} \int_{\omega_{\min}}^{\omega_{\max}} \frac{d\omega}{\omega} \alpha^2 F(\omega) \ln(\omega) \right) \quad \text{(I.14)}$$

and μ_* is the Coulomb pseudopotential, for which we used widely accepted lower and upper bound values of 0.10 and 0.15. [15]

Crystal structures of the predicted phases were generated using VESTA software.

I.6 Critical temperature by McMillan T_C:

Solving the Eliashberg system, even in the isotropic form, is a quite demanding task. However, the most relevant results can be obtained using a simpler approach proposed by McMillan. Through a fit of a large set of results obtained using the spectral function of lead and solving the Eliashberg equations in a small range of the parameter space (λ<2 and μ_*<0.15), McMillan obtained an analytic formula for the critical temperature:

$$T_C = \frac{\Theta_D}{1.45}\exp\left[-\frac{1.04(1+\lambda)}{\lambda-\mu^*(1+0.62\lambda)}\right] \quad \text{(I.15)}$$

Where Θ_D is the Debye temperature and the number λ has the same meaning as the electron phonon coupling parameter, and can be derived from the Eliashberg function as

$$\lambda = 2\int d\Omega \frac{\alpha^2 F(\Omega)}{\Omega} \quad \text{(I.16)}$$

Later, this formula was refined by Allen and Dynes, who substituted the factor $\Theta_D/1.15$ with $\Omega_{log}/1.2$, with the much more representative frequency

$$\Omega_{\log} = \exp\left[\frac{2}{\lambda}\int d\Omega \log\Omega \frac{\alpha^2 F(\Omega)}{\Omega}\right] \quad \text{(I.17)}$$

Which is a weighted average of the phonon frequencies. The McMillan formula predicts an upper limit for T_C even if λincreases indefinitely. However this was a wrong conclusion because the equation (43) was not derived analytically but obtained by numerical solutions in a fixed range of the coupling constant and then it is not possible to consider the limit for $\lambda! 1$. For $\lambda/1$, taking the limit of the Eliashberg equations the following expression for T_C can be obtained in an analytical way

$$T_C = 0.183\omega_D\sqrt{\lambda} \quad \text{(I.18)}$$

and it is clear that in Eliashberg theory there is no upper limit for the critical temperature. In general, the Eliashberg equations are solved numerically with an iterative method until you reach self-consistency. The numerical procedure is very simple in the formulation on imaginary axis; much less so on the real one. The critical temperature can be calculated or by solving an eigenvalue equation [8] or, more easily, by giving a very small test value to superconducting gap (for the Pb it is Δ = 1.4 meV at T = 0 K so, for example, $\Delta(T) = 10^{-7}$ meV) and checking at

which temperature the solution converges. In this way, T_c is obtained with accuracy superior to experimental error bars.

I .7 Applications:

Despite the fact that superconductors need to be cooled down to cryogenic temperatures to work, they have found their way into the commercial market in different applications[16].

The largest part of the applications consists of superconducting magnets. The reason for this is when comparing a conventional magnet made of copper wire with a superconducting magnet producing the same magnetic field, it would be between 100 – 200 times less heavy than the conventional magnet. In addition, the superconducting magnet can be put in a so-called *persistent mode*. Persistent mode is the possibility to charge a magnet to the desired field strength, and to keep that field only cooling of the magnet is necessary, i.e. the current source producing the field can be shut down. Applications of superconducting magnets can be found in nuclear magnetic resonance (NMR) magnets, they are used in a powerful method in chemistry and biology to identify and study the structure of complex molecules. Another application is the magnets for particle accelerators. In high-energy physics, the superconducting magnets are used to bend the tracks of the particles in circular accelerators. Superconducting magnets are also used as magnetic resonance imaging (MRI) magnets in hospitals where inner parts of the body are imaged, without any surgery. This is by far the largest commercial area of superconducting technology today.

Another large application with superconductors is the *Josephson Effect*, which is the phenomenona where a current floats between two superconductors separated by a thin insulator. The arrangement is known as a Josephson junction, and the current floating between is called Josephson current. A major application of the Josephson effect is the SQUID (Superconducting Quantum Interference Device), which is an extremely sensitive magnetometer[17].

Promising future applications include high-performance electric power transmission, transformers, power storage devices, magnetic levitation devices and many more. However, superconductivity is sensitive to moving magnetic fields so applications that use alternating current (e.g. transformers) will be more difficult to develop than those that rely upon direct current[18].

A one-dimensional SQUID array nonlinear transmission line has been used as a parametric amplifier, tunable for microwave signals between 4 and 8 GHz, and providing up to 28 dB of gain. This amplifier is suitable for use in detecting signals from low temperature qubits operating at microwave frequencies, and can squeeze quantum noise [19].

I.8 Atom Hydrogen Clathrate Structures Hydrides at High Pressures:

Room-temperature superconductivity has been a long-held dream and an area of intensive research. The quest for the holy grail of high-pressure physics, metallic hydrogen, has continued to attract the interest of experimentalists and theorists since Ashcroft proposed that the new phase should exhibit superconductivity with Tc∼270 K [20].

Recent experimental findings of superconductivity at 200 K in highly compressed hydrogen (H) sulfides have demonstrated the potential for achieving room-temperature superconductivity in compressed H-rich materials [21].

It has been suggested that at high pressures the lightest element, H, forms metallic solids with the high Debye temperature and strong electron-phonon coupling necessary for high-Tc phonon-mediated superconductivity The superconductivity is supported by a number of calculations that have predicted a high Tc in the range 100–760 K in either molecular or atomic phases . Unfortunately, low temperature studies up to 388 GPa have not yet realized metallization of solid hydrogen. Metallization of solid H at 495 GPa has recently been reported, but additional experimental measurements are required to verify this claim. H-rich materials have been considered as an alternative, because they can metallize at much lower pressures than are accessible to experiments. Extensive theoretical studies have explored potential superconductivity in compressed H-rich materials. Encouragingly, the results suggest the possibility of high-Tc superconductivity in hydrides with estimated Tc values in the range 50–264 K. The subsequent experimental observation of high-Tc superconductivity in the temperature ranges 30–150 K and180–203 K for various temperature-annealed samples in highly compressed H_2S is remarkable. These experiments were motivated by a theoretical prediction of high-Tc superconductivity in compressed solid H_2S, which excluded the possibility of the dissociation of H_2S into S and H and opened up the possibility of synthesizing superconducting H_3S via compression of H_2S. Two properties of metallic hydrides are particularly beneficial for promoting high-Tc superconductivity: (i) a large H-derived electronic density of states at the Fermi level, and (ii) large modifications of the electronic structure in response to the motion of the H atoms (electron-phonon coupling). It appears to be important to satisfy both of these criteria in hydrides with high H content in order to achieve high Tc values. However, the strategy of pursuing the highest possible H content may not always be the best solution. In reality, a number of hydrides with higher H content (e.g., AsH_8, MgH_{12}, and LiH_8,etc.)

have been found not to exhibit higher Tc values than those containing relatively less H, such as CaH_6 and YH_6. The key drawback of these H-rich structures lies in the appearance of H_2-like molecular units that attract many electrons from H atoms with low-lying energies away from the Fermi energy, which violates both criteria (i) and (ii). Another desirable property that is important for achieving high-Tc superconductivity is that the structures should have high symmetry. This appears to be a very general property that is not confined to metallic hydrides[22].

Superconductivity of binary hydrides viewed through the Periodic Table.

Table I.1. Mendeleev table with already investigated binary XHn, where the numbers are maximum calculated Tc. The data were taken from sources given in Table I.3.

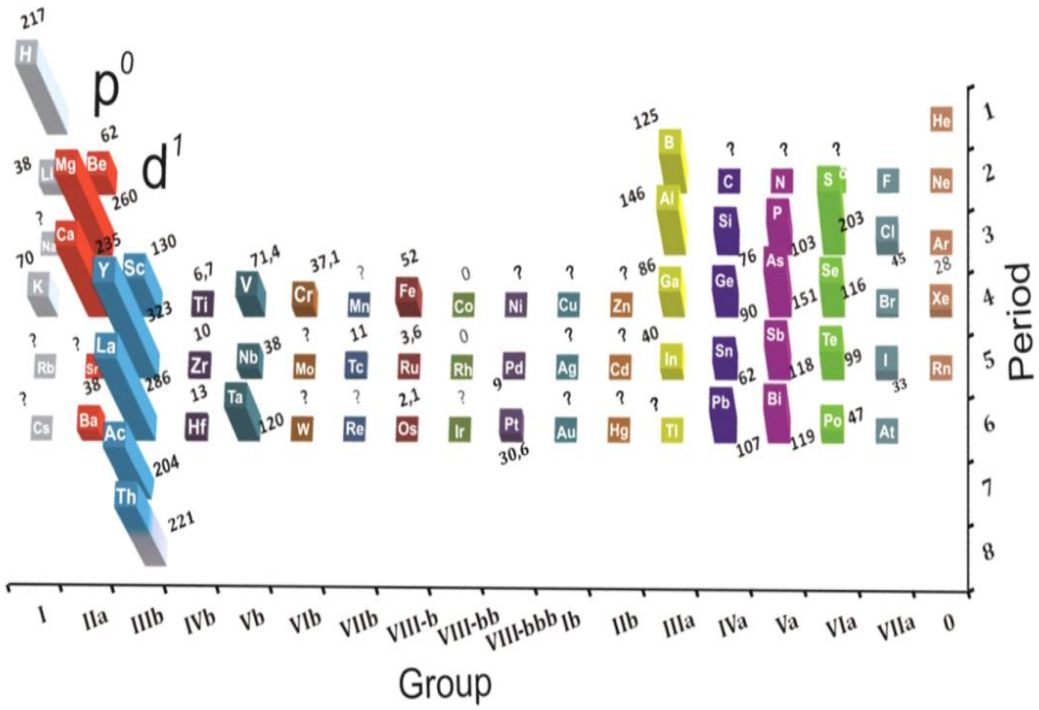

Table I.2. Previously predicted or synthesized binary hydrides with maximum T_C values, which were used [22].

Hydride (Pressure, GPa)	**max Tc, (K)**	**Hydride (Pressure, GPa)**	**max Tc, (K)**	**Hydride (Pressure, GPa)**	**max Tc, (K)**
H solid (500)	217	HfH2(260)	13	AlH5 (250)	146
LiH6 (150)	38	VH8(200)	71.4	GaH3(160)	86
KH6(166)	70	NbH4(300)	38	InH3(200)	40
BeH_2(400)	62	TaH6(50)	120	Si2H6(362)	79
MgH6(300)	260	CrH3(81)	37.1	GeH8(250)	90
CaH_6(150)	**235**	TcH2(200)	11	SnH4(200)	62
BaH_6 (100)	38	FeH5(150)	52	PbH8(230)	107
ScH_6(285)	130	RuH3(100)	3.6	PH3(207)	103
YH10(300)	323	OsH (100)	2.1	AsH8(350)	151
LaH10(300)	286	CoH3	0	SbH4(150)	118
AcH10(200)	204	RhH	0	BiH5(300)	119
ThH10(100)	221	PdH (0)	9	H3S (155)	203
TiH2(0)	6.7	PtH (76)	30.6	H3Se (200)	116
ZrH (120)	10	BH3(360)	125	H4Te (200)	99

I.9 The crystalline structure:

cI14 prototype of CaH_6 becomes the global optimal structure of CaH_2n (n=1-6) at pressure of approximate 150 GPa. With space group Im-3m structures are the most stable forms at the pressures of 50, 100 and 150–300 GPa. in this structure the Ca atoms locate at (0.0.0) and H atoms at (0.25,0,0.5).

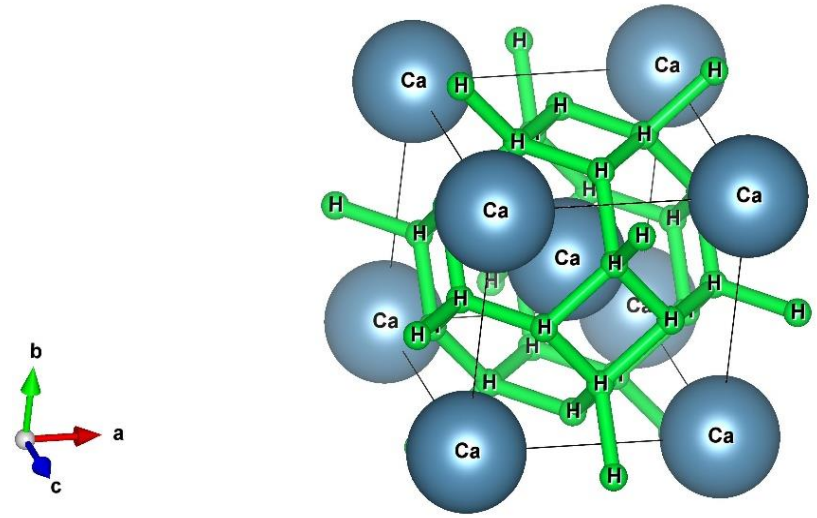

Figure I.7 A 1×2×2 supercell of cI14-CaH_6 at 150 GPa.

I.10 Summary:

Superconductors are the materials, which show a sudden drop of electrical resistance at a certain temperature when cooled below room temperature. While most superconductors of early generation were low T_C materials, next generation superconductors, layered oxides based on perovskite structure, were called as high T_C as materials showing T_C in the excess of liquid N_2 temperature. These have been successfully fabricated in various forms and examined at various places across the world. While the BCS theory explains the origin, the superconductivity in the low T_C superconductors quite well, a well agreed theory for the high T_C ceramic oxides is yet to evolve. These have found applications in magnetically levitated trains and magnetic resonance imaging for medical applications.

References.

[1] "W.Meissner and R. Ochsenfeld, Naturwissenschaften 21, 787 (1933)."

[2] V. Kauppila, *Flat-band superconductivity and heat transport in superconductors*. Aalto University, 2017.

[3] F. London and H. London, "The electromagnetic equations of the supraconductor," *Proc R Soc Lond A*, vol. 149, no. 866, pp.

[4] R. Wesche, "Brief History of Superconductivity," .

[5] D. van Delft and P. Kes, "The discovery of superconductivity," *Phys. Today*, vol. 63, no. 9, pp. 38–43, Sep. 2010.

[6] A. C. Rose-Innes and joint author.) Rhoderick E. H., *Introduction to superconductivity*, [1st ed.]. Oxford ; New York : Pergamon Press, 1969.

[7] W. Meissner and R. Ochsenfeld, "Ein neuer Effekt bei Eintritt der Supraleitfähigkeit," *Naturwissenschaften*, vol. 21, pp. 787–788, Nov. 1933.

[8] W. Wang, "An investigation into high temperature superconducting flux pump technology with the circular type magnetic flux pump devices and YBaCuO films," Thesis,

[9] B. Espinosa Arronte, Kungliga Tekniska högskolan, and Institutionen för mikroelektronik och tillämpad fysik, "Resistivity and the vortex solid-to-liquid transition in high-temperature

[10] M. Tinkham, *Introduction to Superconductivity*. Courier Corporation, 1996.

[11] S. Khene, *Critical Currents and Superconductivity: Ferromagnetism Coexistence in High-Tc Oxides*. CRC Press, Taylor & Francis Group, 2016.

[12] Joe Khachan and Stephen Bosi, *Superconductivity*.

[13] "A. E. Karakozov, E. . Maksimov, and A. A. Mikhailovskii, JETP 75, 70 (1992)."

[14] "N. A. Kudryashov, A. A. Kutukov, and E. A. Mazur, ZhETF 151, 165 (2017)."

[15] Momma, K.; Izumi, F., "VESTA 3 for Three-Dimensional Visualization of Crystal."

[16] S. M. Anlage, "The physics and applications of superconducting metamaterials," *J. Opt.*, vol. 13, no. 2, p. 024001, Feb. 2011.

[17] J. W. Bray, "Superconductors in Applications; Some Practical Aspects," *IEEE Trans. Appl. Supercond.*, vol. 19, pp. 2533–2539, Jun. 2009.

[18] N. Lazarides and G. P. Tsironis, “rf superconducting quantum interference device metamaterials,” *Appl. Phys. Lett.*, vol. 90, no. 16, p. 163501, Apr. 2007.

[19] Tunable coupling of transmission-line microwave resonators mediated by an rf SQUID

Friedrich Wulschner,Jan Goetz,Fabian R Koessel,Elisabeth Hoffmann,Alexander Baust,

[20] N. W. Ashcroft, Phys. Rev. Lett.21, 1748, 1968.

[21] A. P. Drozdov, M. I. Eremets, I. A. Trojan, V. Kseno-fontov, and S. I. Shylin, Nature 525, 73, 2012

[22] article “Dmitrii V. Semenok*, 1,2 Alexander G. Kvashnin AcH 16 as hightemperature conventional superconductors.

Chapter II:

Ab-initio methods

Chapter II: Ab-initio methods

II.1 Introduction :

Our modern picture of what a material is, on the smallest scale, has its foundation in the early 20th century with the discovery of the atom and the development of quantum mechanics. This picture describes a material as consisting of electrons and atomic nuclei behaving according to the probabilistic predictions of quantum theory. This description gave rise to two competing approaches on how to find the energy of a many electron system. The first approach was to solve the quantum mechanical Schrödinger equation for the movement of the individual electrons and to derive the energies from this procedure, using a many particle wave function of a dimensionality proportional to the number of electrons in the system (which usually is a very large number). In contrast, the other approach focused on the total electron density as a fundamental variable and tried to find a direct relation between this density and the energy of the system. Initially, starting with the work of Thomas and Fermi in 1927 [1], this was seen as a way of obtaining crude approximations to the Schrödinger equation method. This status was greatly improved, however, by Hohenberg and Kohn [2]who in 1964 showed how this approach was theoretically capable of finding as exact energies as the ones obtained from the Schrödinger equation. The resulting theoretical framework was called density functional theory and can be regarded as a method equivalent to solving the Schrödinger equation for the energy but avoids many of the difficulties associated with many electron wave functions.

II.2 The Schrödinger Equation:

The theory of quantum mechanics is one of the most well tested theories in science and it has not yet been proven wrong. The mathematical machinery of the theory may be represented by the time-independent non-relativistic Schrödinger equation [3].

$$\mathrm{H}\Psi = \mathrm{E}\Psi \qquad \text{II-(1)}$$

Where H is Hamiltonian operator given by equation n°II-(2):

$$\mathrm{H} = T_N + T_e + U_{ee} + U_{Ne} + U_{NN} \qquad \text{II-(2)}$$

With:

T_N: The kinetic energy of the nuclei.

T_e: The kinetic energy of the electrons.

U_{ee}: Potential energy of electron-electron repulsion.

U_{Ne}: Potential energy of attraction between nuclei and electrons.

U_{NN}: Potential energy of repulsion nucleus-nucleus.

And:

E: Hamiltonian eigenvalue, it stands for system total energy.

Ψ: Hamiltonian proper function, its which depends on the spatial coordinates of nuclei and electrons. Ψ: $\Psi\left(\{\overrightarrow{R_\iota}\},\{\vec{r_\iota}\}\right)$

We used for the equations of quantum mechanics atomic units which are summarized in the Following table and this will not create problems.

Well in atomic units, the Hamiltonian of system writing as fellow:

$$H=\left[\frac{1}{2}\sum_{j=1}^{N}\frac{1}{M_j}\nabla_j^2-\frac{1}{2}\sum_{i=1}^{Ne}\frac{1}{M_i}\nabla_i^2-\sum_{j=1}^{N}\sum_{i=1}^{Ne}\frac{Z_j}{\left|\overrightarrow{R_j}-\vec{r}_{i\,i}\right|}+\sum_{i=1}^{Ne}\sum_{k>i}^{Ne}\frac{1}{\left|\vec{r}_k-\vec{r}_i\right|}+\sum_{j=1}^{N}\sum_{l>1}^{N}\frac{Z_j}{\left|\overrightarrow{R_l}-\overrightarrow{R_j}\right|}\right] \qquad \text{II-(3)}$$

With:

M_j :j^{th}Nucleus mass.

R_j :j^{th} Nucleus charge.

$\overrightarrow{R_j}$: j^{th} Nucleus vector position.

$\vec{r}_i$: j^{th} Electron vector position.

II.3 Born – Oppenheimer approximation

The Born–Oppenheimer approximation is widely used in quantum chemical calculations. The validity of the Born–Oppenheimer approximation is based on the fact that the nuclei are much heavier and move much slower than the electrons. This means that to a good approximation, the nuclei can be considered to have a fixed geometry since the electrons will instantaneously adapt to every nuclear configuration.

$$\Psi\left(\vec{R},\vec{r}\right)=\Phi_N\left(\vec{R}\right)\times\Psi_e(\vec{r}) \qquad \text{II-(4)}$$

Fixing the nuclei, which may be achieved by considering the nuclear mass to be infinitely large, results in a considerably simplified Hamiltonian operator Eq II-(3) The kinetic energy operator of the nuclei vanish due to the presence of the nuclear mass in the denominator, and since the nuclear coordinates become parameters, the nuclear repulsion potential energy is reduced to a constant

Vnu , and the electron-nucleus attraction potential becomes only parametrically dependent on the nuclear coordinates; then solve system of equations following:

$$\mathrm{H}_e\Psi_e\left(\vec{r},\vec{R}\right) = E_{elec}\Psi_e\left(\vec{r},\vec{R}\right) \quad \text{II-(5)}$$

$$H_N\Phi_N\left(\vec{R}\right) = E_{nucl}\Phi_N\left(\vec{R}\right) \quad \text{II-(6)}$$

Where H_e and H_N are respectively the electronic Hamiltonian and the nuclei Hamiltonian given as:

$$H_e = T_e + U_{ee} + U_{Ne} \quad \text{II-(7)}$$

$$H_N = T_N + E\left(\vec{R}\right) \quad \text{II-(8)}$$

E(R) is the functional electronic energy which defines the potential energy surface of the cores. When the total energy is:

$$E_{tot} = E_{ele} + E_{nucl} \quad \text{II-(9)}$$

And:

$$E_{ele} = \sum_{i=1}^{N_e} \varepsilon_i \quad \text{II-(10)}$$

$\varepsilon_i$it is the energy of the i^{th} electron.

II.4 Hartree approximation

In 1928 Hartree [4] proposed the second approximation which is the ground-state wave function of the many-body system is expressed as simple product of orthonormalzed one electron spin-orbitals in the form:

$$\Psi_e\left(\{\vec{r}_i\},\{\vec{R}_j\}\right) = \prod_{i=1}^{N_e} \Psi_e\left(\vec{r}_i\right) \quad \text{II-(11)}$$

Some consequences of this hypothesis:

Obviously, that the simple Hartree product II-(11) does not have the correct antisymmetric character for the interchange of space and spin coordinates of any two electrons.

The Pauli principle is not respected, avoiding multiple occupancies of any given spin-orbital.

Colombian repulsion is overestimated because the electron interacts with himself.

The Schrödinger equation is writing:

$$\mathrm{H_H}\Psi_e(\vec{r}_i) = \mathcal{E}_i\Psi_e(\vec{r}_i) \qquad \text{II-(12)}$$

The electronic charge density n(r) corresponding to the Hartree wave function (8) is given by:

$$n(\vec{r}) = \sum_{i=1}^{N_e}|\Psi_e(\vec{r}_i)|^2 \qquad \text{II-(13)}$$

When repulsion electron-electron potential (Colombian term) become:

$$U_{ee}(\vec{r}_i) = \int \frac{n(\vec{r}_j)}{|\vec{r}_i - \vec{r}_j|} d\vec{r}_j \qquad \text{II-(14)}$$

II.5 Hartree-Fock approximation

The Hartree method is useful as an introduction to the solution of many-particle system and to the concepts of self-consistency and of the self-consistent-field, but its importance is confined to the history of physics. A better approach, that correctly takes into account the antisymmetric character of the the wave functions is the Hartree Fock approach. The price to pay is the presence in the equations of a non-local, and thus more complex, exchange potential[5].

In Hartree–Fock theory, the wave function is approximated as a Slater determinant

(16)-II
$$\Psi_e(1,2,..,N) = \Psi_{SD}(1,2,..,N) = \frac{1}{\sqrt{N!}}\begin{vmatrix} \psi_1(r_1) & \psi_2(r_1) & \cdots & \psi_N(r_1) \\ \psi_1(r_2) & \psi_2(r_2) & \cdots & \psi_N(r_2) \\ \vdots & \vdots & \ddots & \vdots \\ \psi_1(r_N) & \psi_2(r_N) & \ldots & \psi_N(r_N) \end{vmatrix}$$

Where N is the number of electrons. The Slater determinant represents the simplest form of an anti-symmetrized wave function constructed from a product of molecular orbitals. The Slater determinant satisfies the Pauli principle. Where each wave function Ψ_i is called orbital spin, because it is composed of two parts: a space orbital function and the other is a spin function (up or down). $\frac{1}{\sqrt{N!}}$ is a normalizing factor of the determinant.

After the application of the Hamiltonian H_H on the wave function, we obtain the electronic mono equations of Hartree-Fock:

$$(17)\text{-II} \qquad \left(-\frac{1}{2}\nabla_i^2 + U_{ext}(r,R) + \sum_{\substack{j=1 \\ j\neq i}}^{n} \int \frac{\left|\varphi_j(r')\right|^2}{\left|r-r'\right|} dr' \right) \varphi_i(r) - \sum_{\substack{j=1 \\ j\neq i}}^{n} \int \frac{\varphi_j(r)\varphi_j^*(r')}{\left|r-r'\right|} dr' \varphi_i(r') = \varepsilon_i \varphi_i(r_i)$$

Such as

$-\frac{1}{2}\nabla_i^2$ is the kinetic energy of the electron.

$U_{ext}(r,R)$ is the energy of attraction between nuclei and electrons.

$\sum_{\substack{j=1 \\ j\neq i}}^{n} \int \frac{\left|\varphi_j(r')\right|^2}{\left|r-r'\right|} dr'$ is the integral of Coulomb noted J_{ij} (the potential of Hartree).

$\sum_{\substack{j=1 \\ j\neq i}}^{n} \int \frac{\varphi_j(r)\varphi_j^*(r')}{\left|r-r'\right|} dr'$ is the integral of exchange noted K_{ij}.

The last term is the result of anti-symmetry of the wave function.

II. 6 Density of functional theory

In 1927, Walter KOHN and Pierre HOHENBERG [6] proposed a new idea, which is to replace the multi electronic wave function with electronic density, a simpler and more manageable function. The concept of this idea called DFT (density functional theory) is that the energy of an electronic system can be expressed as a function of the electronic probability density that minimizes the energy of the system .This is actually an old idea dating mainly to the works of Thomas [1] and Fermi [6] expressing all the total energy contributions in terms of the electron density

II.6.1. Kohn-Hohenberg theory

The early efforts to find energy functionals (the Thomas–Fermi model and extensions along the same idea) were all based on “sensible” approximations, which gave decent results when applied to certain real problems. There is a great conceptual difference between these heuristic “guesses” and the elegant analytical framework following the work of Hohenberg and Kohn [6].

The first theorem: either $n(r)$ the density of the system in the fundamental state, there exists only one external potential $V_{ext}(r)$, which can generate it, and the energy of the ground state can be written as a functional of the electronic density:

$$E\left[n(\vec{r})\right] = \langle\psi|H|\psi\rangle = F\left[n(\vec{r})\right] + \int V_{ext}(\vec{r}).n(\vec{r}).d\vec{r} \qquad \text{II-(18)}$$

With
$$F\left[n(\vec{r})\right] = T_e\left[n(\vec{r})\right] + V_{ee}\left[n(\vec{r})\right] \qquad \text{II-(19)}$$

Where $F\left[n(\vec{r})\right]$ is the functional of Hohenberg and Kohn it is common for any electronic system, and 'it depends only on the density [6].

The second theorem: The energy reaches its minimum for the real density (the electronic density of the system in the ground state is that which minimizes the total energy) [6].

$$E\left[n_0(t)\right] \leq E\left[n(t)\right] \qquad \text{II-(20)}$$

II.6.2 The Kohn-Sham equations

Kohn and Sham propose to replace the interacting multi-particle system with a system without interactions that is easier to solve. Kohn and Sham's approach [7]assumes that the ground-state electronic density of the real system is equal to that of another non-interacting particle-free system. This leads to solving a set of equations for independent particles like those of Hartree or Hartree-Fock:

$$H_{KS}\varphi_i(r) = \varepsilon_i\varphi_i(r) \qquad \text{II-(21)}$$

With
$$H_{KS} = -\frac{1}{2}\nabla_i^2 + U_{eff}(r) \qquad \text{II-(22)}$$

And
$$U_{eff} = U_{ext}(r) + \int \frac{n(r')}{|r-r'|}dr' + U_{xc(r)} \qquad \text{II-(23)}$$

The problem is that we can not define the term of exchange and correlation of exact handling, so we have to make approximations.

II.6.3. Local Density Approximation (LDA)

The local density approximation (LDA) assumes that the density of a particle at the point, depends only on the density in, and that it is equal to the exchange energy correlation per particle of a homogeneous gas density:

$$E_{xc}^{LDA}\left[n(r)\right]=\int n(r)\varepsilon_{xc}^{LDA}(n(r))dr \qquad \text{II-(24)}$$

Or the exchange-correlation energy can be decomposed as the sum of the exchange energy and the correlation energy:

$$\varepsilon_{xc}^{LDA}\left[n(r)\right]=\varepsilon_{x}\left[n(r)\right]+\varepsilon_{c}\left[n(r)\right] \qquad \text{II-(25)}$$

The exchange contribution is known, it is given by the exchange energy functional of Thomas-Fermi-Dirac

$$\varepsilon_{x}^{LDA}(r)=-\frac{3}{4}\left(\frac{3}{\pi}\right)^{\frac{1}{3}}n(r)^{\frac{1}{3}} \qquad \text{II-(26)}$$

On the other hand, the correlation energy, which is more complex to evaluate, is usual parameterized from quantum Monte Carlo calculations performed by Ceperley and Alder [8].

II.6.4. Generalized Gradient Approximation GGA

One way to improve the exchange-correlation functional is to take into account the local density $n(r)$ but also the amplitude of its gradient $\nabla n(r)$. Taking into account the density gradient thus makes it possible to account for the inhomogeneous nature of the electron density around the r These functionalities have a semi-local character although they are always described by a central potential and can be written in the general form[9]:

$$E_{xc}^{GGA}\left[n(r),\nabla n(r)\right]=\int n(r)\varepsilon_{xc}^{GGA}\left[n(r),\nabla n(r)\right]dr \qquad \text{II-(27)}$$

At present, the most widely used GGA functionalities are those proposed by Perdew and Wang (PW91)[10], Perdew, Burke and Ernzerhof (PBE) [11], as well as the revised version of PBE proposed by Hammer, Hansen and Norskov (RPBE) [12].

II.7 Pseudo potential method

The pseudo-potentials approach is based on the assumption that most of the physical properties of electronic systems are much more dependent on valence electrons than on core electrons, the bonding of atoms is essentially due to valence electrons while the electrons of heart can be considered frozen and so they can be ignored in most cases.

Practically, the pseudo potentials are constructed so that beyond a certain cut-off radius, defining a sphere within which are located the core electrons, the pseudo-potential and the pseudo-wave functions. Of valence must be identical to the true potential and the true valence wave functions: for $|r| > r_c, V_{pp}(r) = V_{ext}(r)$ and $\psi^{PP}(r) = \psi^{AE}(r)$

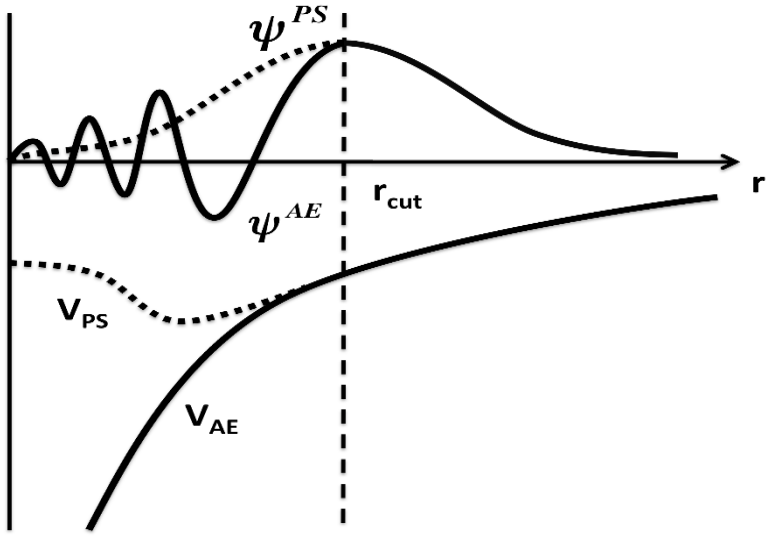

Figure II-1: Schematic representation of the pseudopotential method

The pseudo potential thus makes it possible to reduce the number of electrons to be taken into account in the calculation and also to reduce the number of plane waves necessary to describe the wave functions of the solid. This leads to reducing the calculation volume and shortening the execution time.

II.8 Periodic systems and Bloch's theorem

Bloch's theorem is a consequence of the periodicity of the crystalline potential; it illustrates the invariance of the system by translational symmetry. The wave function is then written as the product of a periodic function, u_j^k specific to the network, and a plane wave, which translates the network translation.

$$\psi_j^k(\vec{r}) = u_j^k(\vec{r})e^{i(\vec{k}.\vec{r})} \qquad \text{II-(28)}$$

$$u_j^k(\vec{r}) = \sum_G \tilde{u}(\vec{G})e^{i(\vec{G}.\vec{r})} \qquad \text{II-(29)}$$

The vectors $\vec{G}$ and $\vec{k}$ are defined in reciprocal space within the first Brillouin zone. The wave vector $\vec{k}$ is a quantum number, specific to Bloch's orbitals. The resolution of the Kohn and Sham equations in a periodic system is necessarily for a finite number of points K obtained by a representative and suitable sampling of the ZB, which reproduces faithfully its symmetry.

II.9 Sampling of the Brillouin zone (BZ)

Several terms in the total energy that are calculated can be expressed in integrals on the Brillouin zone (ZB). On a computer, the integral will be approximated by a weighted sum. The grid of k-points used for this summation must converge and sufficiently dense to represent the variations of the integral. Various methods of sampling the ZB have been proposed, but the most used is Monkhorst and Pack [13].

Many procedures of election exist for the sampling of the k points One will quote in particular those of Chadi and Cohen [14], those of Evarestov et Smirnov[15], or those of Monkhorst [16]et Pack which we are used in this work.

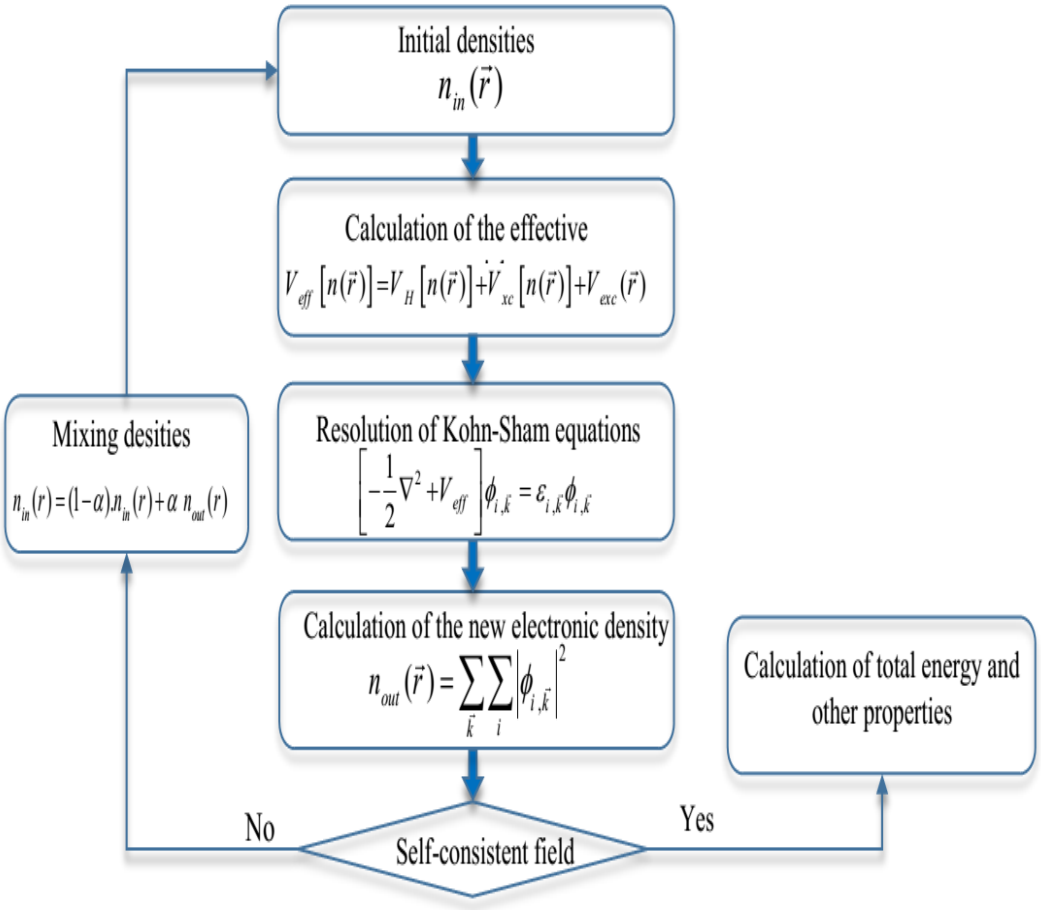

Figure II-2: Flowchart of DFT self-consistent cycle calculation

II.10 Density functional perturbation theory (DFPT)

All the physical properties of a system (a crystal in our case) represent the response of the system to an external disturbance (atomic displacement, electric field, deformation...), then these properties are only the change that the energy undergoes total disturbed system. They are directly related to the derivatives of the total energy with respect to one (or more) perturbation (s)[17].

Many interesting physical properties (response functions) are the result of the application of an external perturbation to the system under investigation. Response functions are first second, third, or higher order derivatives of the total energy with respect to applied perturbation(s). Typical perturbations can be atomic displacements, homogeneous external electric or magnetic fields, strain, alchemical change, etc... The physical properties related to the derivatives of the total energy are:

1st order: forces, stress, dipole moment,...

2nd order: phonon dynamical matrix, elastic constants, dielectric susceptibility, Born effective charges, piezoelectricity, internal strain

3rd order: nonlinear dielectric susceptibility, phonon-phonon interaction, Gruneisen parameters, an harmonic elastic constants, ...

if the Hamiltonian H of a system depends on an arbitrary parameter λ. for a normalized wave function, the first derivative of the energy with respect to a parameter is equal to the expectation value of the corresponding first derivative of the Hamiltonian.

$$H(\lambda)\Psi(\lambda) = \Psi(\lambda)E(\lambda) \qquad \text{II-(30)}$$

$$\frac{\partial E(\lambda)}{\partial \lambda} = \langle \Psi(\lambda) \left| \frac{\partial H(\lambda)}{\partial \lambda} \right| \Psi(\lambda) \rangle \qquad \text{II-(31)}$$

One of its consequences being that in Quantum Mechanics there is a single way of defining a generalized force on eigenstates of the Hamiltonian, associated with the variation of some of its parameters. If we can calculate the ground state total energy of a solid, we can calculate many of properties, which linked to derives of the ground state total energy with respect to perturbation.

Further physical properties - such as entropy or thermal expansion - can be obtained integrating the total energy (or a thermodynamic potential) over phononic degrees of freedom.
Total energy derivatives can be computed using either direct approaches (e.g., finite differences, molecular-dynamics spectral analysis) or perturbative techniques. The former suffer from various limitations such as size effects, ergodicity constraints, commensurability problems or the difficulty to decouple the responses to perturbations of different wavelength. The perturbative theory applied to DFT, instead, allows one to treat not only periodic perturbations but also perturbations characterized by a non-zero, commensurate or incommensurate, wavevector [9]. In addition, the computation of 1 st
order corrections to wavefunctions within perturbation theory
can be done using a variational approach (Section 2.3) and algorithms similar to those used for ground-state (i.e. unperturbed) calculations. Hence, the perturbative technique can be naturally included in the usual DFT framework. In the following, unless otherwise specified, we will use Hartree atomic units ~ = m e = e = 1/4πε 0 = 1

Reference

[1] *L. H. Thomas, Proc. Camb. Philos. Soc. 23, 542 (1927); E. Fermi, Rend. Acad. Naz. Lincei6, 602 (1927). .*

[2] "P. Hohenberg and W. Kohn, Phys. Rev. Lett. 136B864 (1964)."

[3] *K. G. Dyall and K. Fægri Jr. Introduction to relativistic quantum chemistry. Oxford University Press., Oxford, 2007. .*

[4] "A. Mickiewie, 'A new formulation,' vol. 111, no. 5, pp. 217–219, 1985."

[5] the Hartree-Fock Method J. C. Slater Phys. Rev. 81, 385 – Published 1 February 1951

[6] *E. Fermi. Rend. Accad. Naz. Lincei 6, (1927) 602. .*

[7] *W. Kohn, L. J. Sham. Phys. Rev 140, (4A) (1965) 1133.*

[8] "D.M. Ceperley, B.J. Alder. Phys. Rev. Lett. 45, (1980) 566."

[9] *C. COMBELLES, thèse de doctorat, Modélisation ab-initio Appliquée `a la Conception de Nouvelles Batteries Li-Ion, université Montpellier II, 2009. .*

[10] "Generalized gradient approximation made simple JP Perdew, K Burke, M Ernzerhof - Physical review letters, 1996 - APS."

[11] "Perdew, burke, and ernzerhof reply JP Perdew, K Burke, M Ernzerhof - Physical Review Letters, 1998 - APS."

[12] "Improved adsorption energetics within density-functional theory using revised Perdew-Burke-Ernzerhof functionals B Hammer, LB Hansen, JK Nørskov - Physical Review B, 1999 -

[13] *H .J. Monkhorst and J .D. Pack, Phys. Rev. B. 1976, 13 (12), 5188. .*

[14] "D. J. Chadi and M. L. Cohen, 'Special points in the brillouin zone,' Phys. Rev. B, vol. 8, no. 12, pp. 5747–5753, 1973."

[15] "R. a Evarestov and V. P. Smirnov, 'Special points of the Brillouin zone and their use in the solid state theory,' Phys. Status Solidi, vol. 119, pp. 9–40, 1983."

[16] "J. D. Pack and H. J. Monkhorst, ''special points for Brillouin-zone integrations'-a reply,' Phys. Rev. B, vol. 16, no. 4, pp. 1748–1749, 1977."

[17] "B .LAGOUN. Thèse de Doctorat. CALCUL ab-initio DES PROPRIÉTÉS P HYSIQUES DE QUELQUES NOUVEAUX MATERIAUX POTENTIELS

Chapter III:
Results and Discussions

III. Results and Discussions

III-1. Introduction

In this chapter, we present and discuss our results of calculations such as the structural properties, the dispersion of phonons, Critical temperature under different pressures and electronic properties at 200 Gpa of CaH_6 with cI14 prototype described in chapter I.

III .2. Calculation method

We have undertaken first principles calculations of cubic body center of CaH_6 with space groups cI14. Our computational calculations are carried out within first-principles approximations in the framework of DFT and DFPT [1] implemented in the ABINIT code [2]. The wave function describes only the valance and conduction electrons, while the core electrons are taken into account within the pseudopotential approximations. First-principles density functional computations were performed within the GGA-PBE. The kinetic energy for the plane-wave basis set has been used as 40 Hartrees, with 8×8×8 converged Monkhost-Pack k-point meshes. The norm-conserving pseudopotentials include semi-core states of *Ca* ($4s^2$**)** and *H* ($1s^1$**)** as a valences states.

III-3. The structural properties

In order to study the pressure as a function of the volume we have first to get the optimal volume at zero pressure. To do this, we have performed a geometric optimization of volume at zero pressure of the volume (figure **III.1)**. An optimized structure corresponds to a minimal energy. To reach this structure, one must calculate the variation of the energy according to the volume of the mesh.

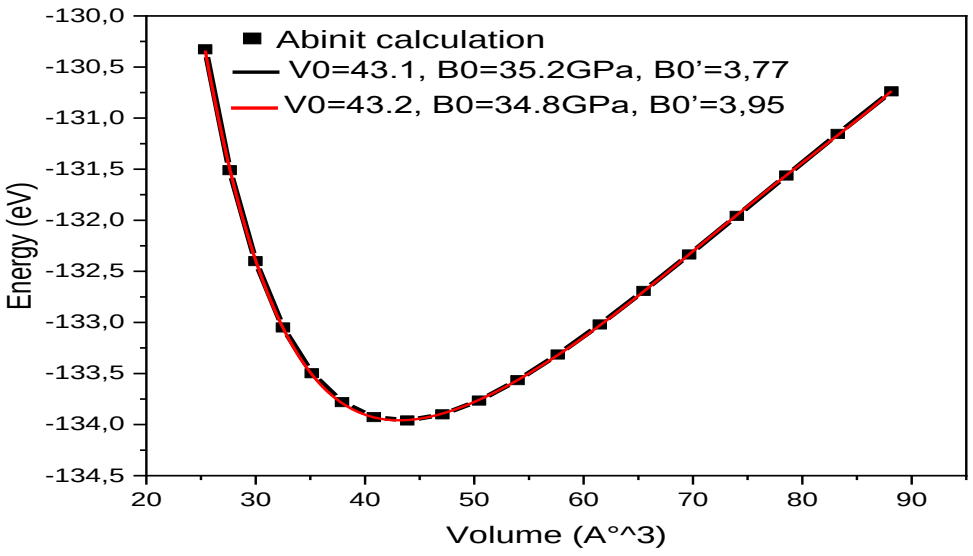

Figure III.1 Variation of total energy as a function of volume for the CaH_6

Figure III.2 presents the compressibility curves, at all pressures the structures of CaH_6 compound exhibit different compressibilities. This study is based on the third order Birch–Murnaghan isothermal equation of state is given by [3] :

$$P(V)=\frac{3B_0}{2}\left[\left(\frac{V_0}{V}\right)^{\frac{7}{3}}-\left(\frac{V_0}{V}\right)^{\frac{5}{3}}\right]\left\{1+\frac{3}{4}\left(B_0^{'}-4\right)\left[\left(\frac{V_0}{V}\right)^{\frac{2}{3}}-1\right]\right\}. \qquad \text{III-(1)}$$

Where P is the pressure, V0 is the reference volume, V is the deformed volume, B0 is the bulk modulus, and B0' is the derivative of the bulk modulus with respect to pressure. The bulk modulus and its derivative are usually obtained from fits to experimental data and are defined

as $$B_0=-V\left(\frac{\partial P}{\partial V}\right)_{P=0}$$ et $$B_0^{'}=\left(\frac{\partial B}{\partial P}\right)_{P=0}$$ III-(2)

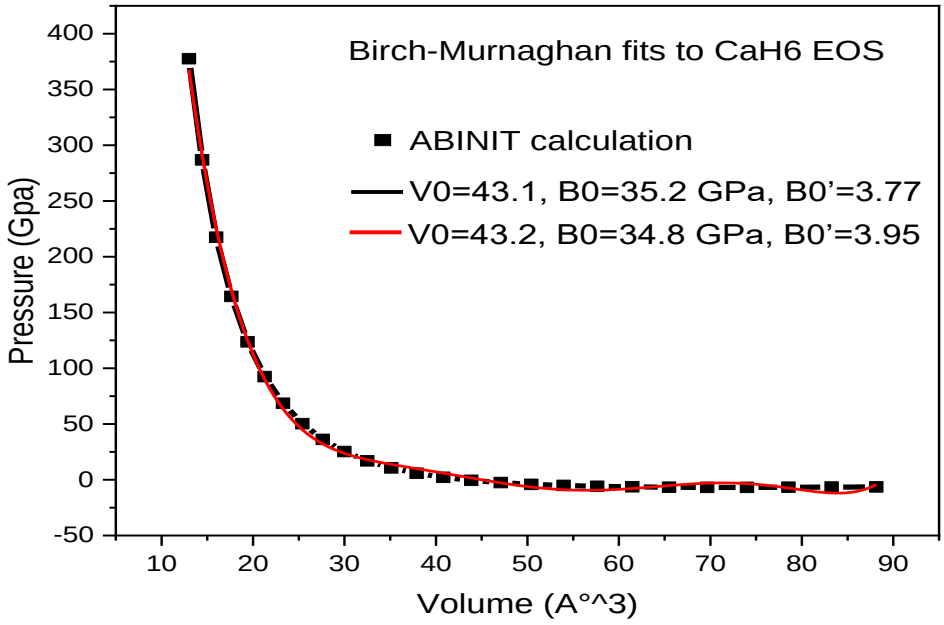

Figure III.2 Variation of total Pressure as a function of volume for the CaH_6 compound.

The table III.1 illustrastes the lattice parameters under different pressures (from 0 to 300Gpa).

Table III.1 lattice parameters *a* (A°) under different pressures

P(Gpa)	*Other work*	*This work*
0	**-**	**4.4171**
10	**-**	**4.1376**
20	**-**	**3.9793**
50	**-**	**3.7041**
75	**-**	**3.5636**
100	**-**	**3.4620**
150	**3,501**[4]	**3.3134**
200	**-**	**3.2049**
250	**-**	**3.1196**
300	**-**	**3.0511**

III-4. The phononic dispersion

Phonon calculations can provide a criterion for crystal dynamical stability and indicate structural stability through non-appearance of negative frequencies. To carry out a rigorous analysis of the dynamic stability, we have determined a systematic study of the lattice dynamics using the DFPT method for different pressure values, which are 150 Gpa, 200 Gpa and 250 Gpa. However, in reference [4] authors found severe imaginary phonons at 150 GPa, eliminating its existence. The presence of the imaginary phonon frequencies indicates the instability of compound. Our results represented on the figure III.3**,** we observe that structure is dynamically stable at pressure more or less 200 Gpa. There is no band gap between the acoustic and optical modes in the stable case unlike other pressures.

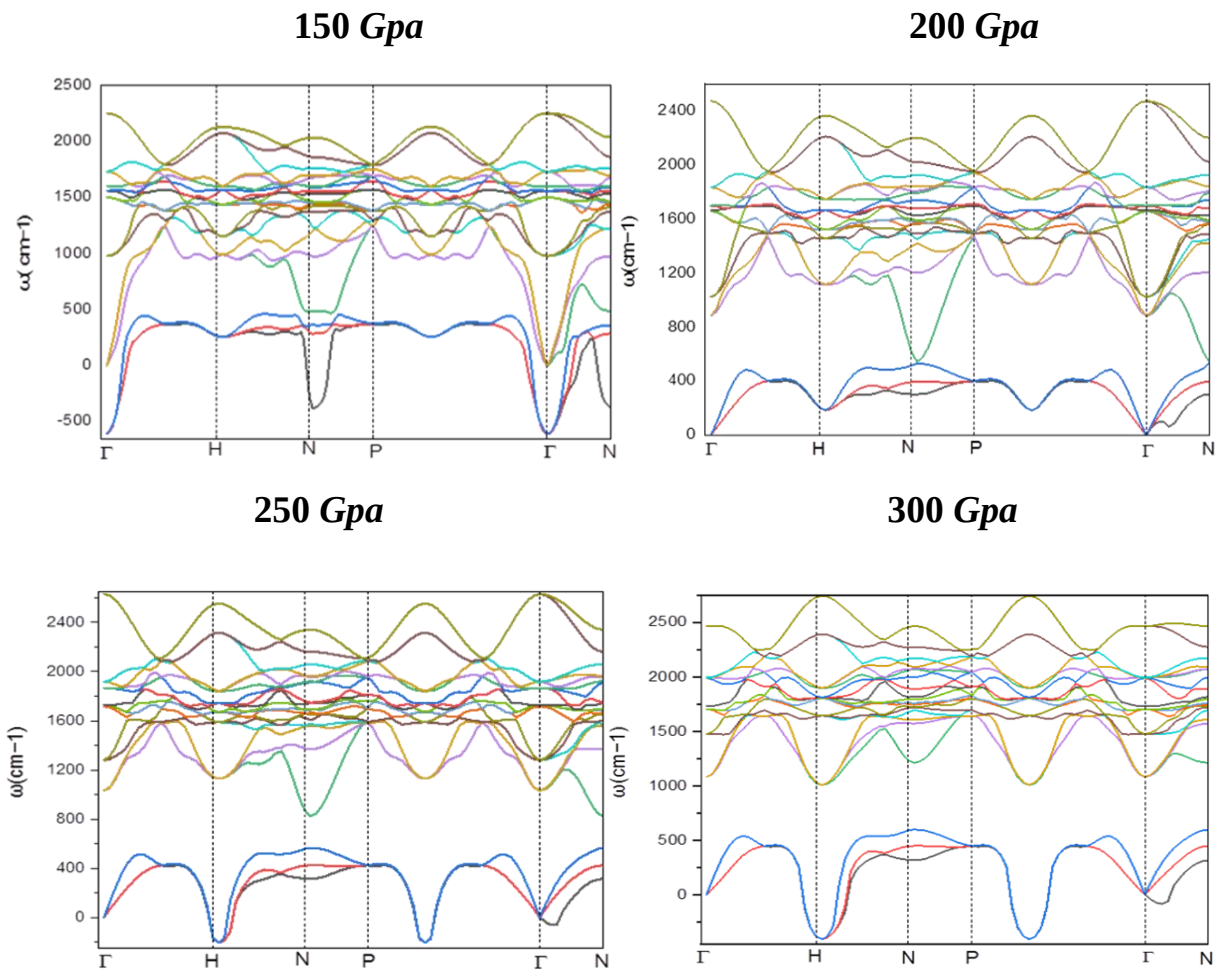

Figure III.3 Phonon band structure of cI14-CaH_6 at 150, 200, 250 and 300 Gpa.

In order to fully understand the phonon band structure at 200 Gpa are accomplished by the diagrams of the density of states TDOS and PDOS (Figure **III.4**). The first region of the interval [113, 561] cm^{-1}: this region is characterized mainly by the movement of the Ca atom and partly by the motions of the H atoms. The second region of the interval [1010, 2427] cm^{-1}: is due mainly to the motion of the atom of H, and partly to the motion of the atom of Ca.

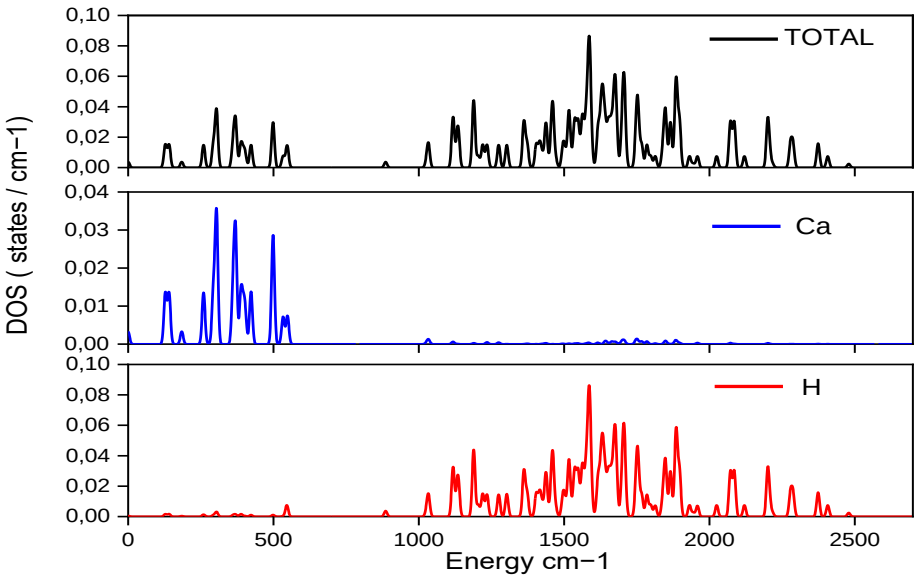

Figure III.4 Calculated total and partial phonon DOS of cI14-CaH_6 at 200 GPa.

III-5. The critical temperature

Among the most important properties in the super conductance field is the critical temperature, which separates the normal state from the superconducting state. Our computations based on Allan–Dynes and McMillan analytical formulas [5] have estimated the T_c for different pressures. the obtained results for this property are summarized in table III.2. Our analysis show that this superconductor exhibits a high T_c values which decreases from 194,59 to130,6 K as the pressure increases from 150 to 250 Gpa. We note that we have used 0,136 the value of $\mu^*$is the Coulomb pseudopotential [15].

Table III.2 The critical temperature T_c (K) under different pressures.

pressure(Gpa)	Other work	This work
150	235 [4]	194.597
200	-	154.247
250	-	130.606

III-6. Electronic properties at 200 Gpa

III-6-1. Band structure

By definition, the structure of the bands is a modeling of the energy values that can take the electrons of a solid inside of it. In a general way, these energies have the possibility of taking values in certain intervals, namely the permissible bands "valence band" and "band of conduction" which are sometimes separated by banned energy bands. Based on this description, it is possible to explain schematically electrical behavior of certain compounds and classify them as insulators, conductors or semiconductors depending on how these bands are distributed. We calculated the band structure in the primitive cell of the cI14 prototype of the CaH_6 system at 200 Gpa. The results obtained are illustrated in Figure (III-5).

The structure of cI14-CaH_6 energy bands in the centered Cube phase calculated according to the points of high symmetry Γ (0, 0, 0), H (0.5, 0.5, 0.5), N (0.0, 0.0, 5), P (0.25.0.25, 0.25), Γ (1, 1, 1), N (1, 1, 0.5).

In the CaH_6 compound phase, the energetic bands of the CaH_6 layers are dominant near the Fermi level, with a large overlap between the valence and conduction bands, allowing electrons to pass directly from the valence band to the band conduction and flow throughout the solid. Therefore, we can say that this system have metallic behavior.

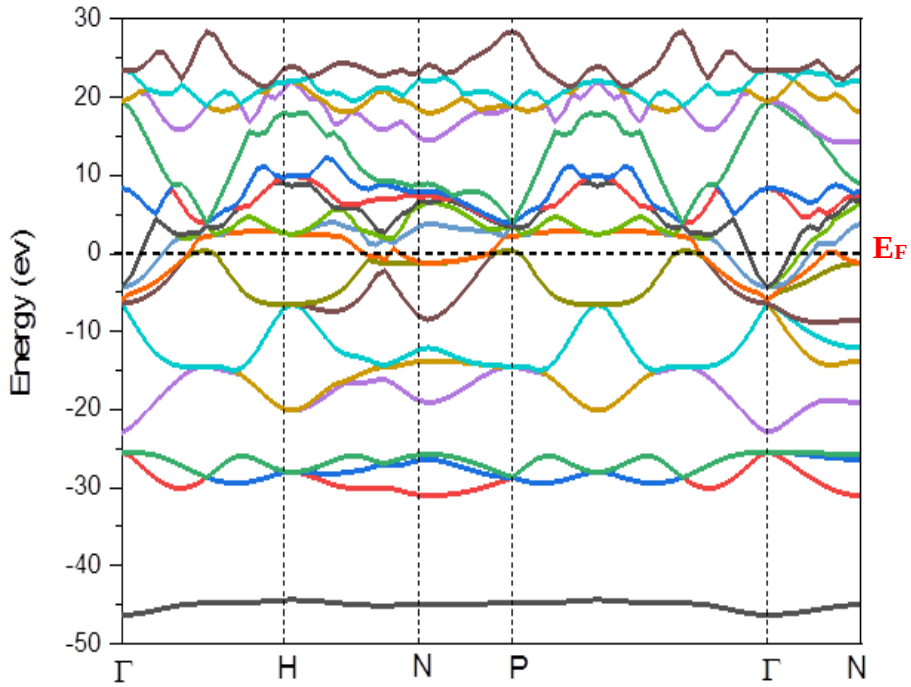

Figure III.5: band structure of the CaH_6 compound at 200 GPa.

III-6-2. Density of states diagrams

We calculated total and partial density of states of the cI14-CaH_6 compound which is Which is considered as a dropping of the band structures. We have reduced the Fermi level to the origin of energies and the results are illustrated in Figure (III-6). From this diagrams we can distinguish three regions:

- The first region is represented the lowest energies betwen -32 eV to 29 eV, it is characterized by the contribution of the 4s states of the Ca atoms which show stronger intensities and small contribution of hydrogen atoms.
- The second area is Fermi level neighborhood, this part is dominated mainly by strong hybridization between Ca-3d orbitals and H-1s, the latter leads to the appearance of a peak in the vicinity of the Fermi energy.
- The third region is above Fermi level it characterized by significant contributions of 1s states of H atoms.

By analyzing the band structure and the density of states, we can notice that the valence states are divided into two: an inner part (of bands), which is in the intervals [-31.77, -29.69], [-16.03, -10.7] and [-6.11, 14.17] eV and which are due to the following states: 4s of Ca and 1s of H for the first band, the second region consists essentially of 1s of H and partially of 3p of Ca, These states are responsible for the Ca-H strong binding (Short). The third part consists largely of 1s of H and a less important way of 3p of Ca.

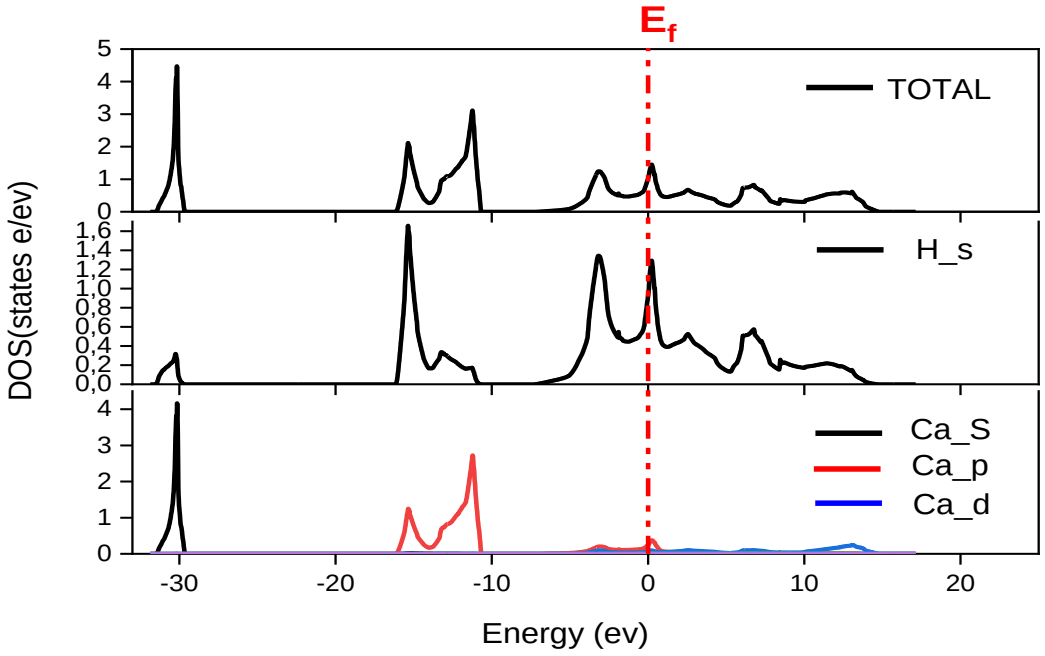

Figure III.6 Density of the states (total and partial) of cI14-CaH_6 at pressure of 200Gpa.

III-7. Conclusion

In this chapter, we have presented our results of calculations based on DFT and DFPT framework for body center of CaH_6 with space groups cI14, which appears under high-pressure. Using ABINIT code, we have studied the pressure as a function of volume, the vibrationel properties under different pressures and electronic properties at 200 Gpa.

References

[1] P. de Giannozzi, S. Gironcoli, P. Pavone, S. Baroni, *Phys. Rev.* B **43**, 7231, 1991.

[2] X. Gonze, et al, *Z. Kristallogr*. **220**, 558, 2005.

[3] P.T. Wedepohl, *Solid State Communications*, vol. 10, 1972, p. 947-951.

[4] H. Wang, J. S. Tse, K. Tanaka, T. Iitaka, and Y. Ma, *Proc. Natl. Acad. Sci.*, vol. 109, no. 17, 2012.

[5] W.L. McMillan, *Phys.Rev*.167, 331, 1968.

[6] G.M. Eliashberg, *Soviet.Phys. JETP*, 11, 696, 1960.

General conclusion

General conclusion

Recent theoretical studies on achieving high-pressure superconductivity are published. Hydrogen-rich compounds hold promise as high-temperature superconductors under high pressures. Through a systematic investigation of CaH_6 with space group cI14, which appears under high-pressure, using DFT and DFPT framework. Based on ABINIT package, we have studied the pressure effects on the structure of this compound. Afterward, we have predicted the phonon's behavior under various pressures and finally, we have studied the electronic properties in stable case. In this manuscript we have shown that:

- From phonon band structure under pressure of 150, 200, 250 and 300 Gpa, We conclude that cI14-CaH_6 compound is stable under 200 Gpa.
- The critical temperatures calculated are 194.597, 154.247 and 130.606 under 150, 200 and 250 respectively. Those values make this compound a potentiel superconductors material with a high T_c
- The band structure and density of states diagrams confirm the metallic behavior of the studied compound.

prospects

Finally, this study paved the way to some future aspirations as the calculation of critical temperature for this compound from other approximations as green function formula and the Fermi surface comportment. We expect to extend this study to others compounds.

الملخص

إن الهدف من هذا العمل هو حساب أولي لخصائص الفيزياء: الهيكلية، والإلكترونية والتذبذبية لـCaH_6 ، والتي تعد واحدة من الموصلات الفائقة الجديدة التي تسمى هيدريد الكالسيوم عند الضغوط العالية. تم إجراء الحساب في إطار النظرية الوظيفية للكثافة (DFT) ، وتم إجراؤها باستخدام برنامج المصدر المفتوح ABINIT ، باستخدام علاقة GGA التبادلية المحتملة التي تم تحديدها بواسطة Perdew و Burke و Enzerhof (PBE). من خلال تطبيق نظرية اضطراب الكثافة الوظيفية (DFPT) ، يمكن أيضًا دراسة استجابة مادة صلبة إلى اضطرابات مثل الحقول الكهربائية أو ذرات الإزاحة. تم التعليق على النتائج التي تم الحصول عليها ومقارنتها بالبيانات التجريبية المتاحة.

كلمات البحث: الخصائص الفيزيائية، الموصلية الفائقة، هيدريد الكالسيوم، DFT، ABINIT، GGA، PBE، DFPT

Abstract

The objective of this work is an ab initio calculation of the physicals properties: structural, electronic and Vibrational of CaH_6, which is one of the new superconductors called clathrate calcium hydride at high pressures. The calculation was conducted in the framework of the functional theory of density (DFT), and it have been performed with the ABINIT open source software, using the potential exchange-correlation GGA parameterized by Perdew, Burke and Enzerhof (PBE). By applying the density-functional perturbation theory (DFPT), one can also study the response of a solid to disturbances like electric fields or the displacement atoms. The results obtained were commented and compared with the available experimental data.

Keywords: physicals properties, superconductor, clathrate calcium hydride, DFT, ABINIT, GGA, PBE, DFPT

Résumé

L'objectif de ce travail est un calcul ab-initio des propriétés physiques : structurelle, électronique et vibratoire de CaH_6, qui est l'un des nouveaux supraconducteurs appelés hydrure de clathrate de calcium à haute pression. Le calcul a été réalisé dans le cadre de la théorie fonctionnelle de la densité (DFT), et il a été réalisé avec le logiciel open source ABINIT, en utilisant le GGA potentiel d'échange-corrélation paramétré par Perdew, Burke et Enzerhof (PBE). En appliquant la théorie de perturbation fonctionnelle-densité (DFPT), on peut également étudier la réponse d'un solide à des perturbations comme les champs électriques ou les atomes de déplacement. Les résultats obtenus ont été commentés et comparés aux données expérimentales disponibles.

Mots-clés : propriétés physiques, supraconducteur, hydrure de clathrate de calcium, DFT, ABINIT, GGA, PBE, DFPT